Chemical Physics Letters 892 (2026) 142796

Contents lists available at ScienceDirect

Chemical Physics Letters

journal homepage: www.elsevier.com/locate/cplett

# Kinetically controlled polymorphism and amorphization of 1-methylpiperidine under high hydrostatic pressure

Qingqing Yang [a], Chaosheng Yuan [a,*], Chenran Zhang [a], Xuerui Cheng [a], Haining Li [a], Yongfu Liang [a], Zheng Wang [a], Xiang Zhu [a], Lei Su [b,c,**]

[a] Electronic information school, Zhengzhou University of Light Industry, Zhengzhou, Henan 450002, China
[b] Shanghai Advanced Research in Physical Sciences, Shanghai 201203, China
[c] Center for High Pressure Science and Technology Advanced Research, Beijing 100093, China

ARTICLE INFO

*Keywords:*
1-Methylpiperidine
Phase transition
Polymorphism
Kinetic effects
Raman spectroscopy

ABSTRACT

Phase transformations of 1-methylpiperidine under static and dynamic compression up to 21 GPa were investigated via in-situ Raman spectroscopy in a diamond anvil cell. Static compression reveals at least three crystalline phases and an amorphous state, which are kinetically sensitive and metastable. Dynamic compression rapidly induces amorphization, and subsequent decompression leads to spontaneous crystallization through Phase III and Phase II. The high-pressure phase behavior of 1-methylpiperidine is kinetically controlled rather than purely thermodynamic, governed by structural evolution, molecular flexibility, and metastable state formation.

## 1. Introduction

1-Methylpiperidine, a vital six-membered nitrogen-containing heterocyclic compound, holds significant application potential across organic synthesis, medicinal chemistry, and materials science [1–3]. This compound presents as a colorless liquid at ambient temperature and pressure [4]. The inherent *N*-methyl substituent, coupled with the rigid six-membered ring framework, confers a distinctive spatial configuration onto the molecule [5]. While the single-crystal structure of 1-methylpiperidine under atmospheric pressure has not been explicitly detailed, structural analyses of related piperidine derivatives strongly suggest a predominant chair conformation for its six-membered ring [6–10]. Intermolecular aggregation is primarily governed by van der Waals forces and weak polar interactions [11]. These structural attributes not only contribute to the compound's excellent solubility and reaction selectivity but also facilitate diverse phase transition behaviors under external pressure manipulation. Such transitions are often intrinsically linked to molecular conformational rearrangements and the dynamic reconstruction of intermolecular interactions, including hydrogen bonding and van der Waals forces.

Unlike regulatory approaches such as temperature and concentration, applied high hydrostatic pressure can effectively compress intermolecular distances, modify the degree of molecular orbital overlap, and thereby modulate the strength and character of intermolecular interactions. This modulation can facilitate transitions of substances from thermodynamically stable states to metastable states or novel stable states under pressure [12–17].

A growing body of research has explored the impact of high pressure on piperidine and related nitrogen-containing heterocyclic compounds. For instance, Tafazzoli et al. [18] employed pressure-temperature dependent gas-phase proton nuclear magnetic resonance ($^1$H NMR) spectroscopy. Their findings revealed that elevated pressure significantly alters the energy barrier associated with the ring-flipping isomerization of the six-membered ring in 1-methylpiperidine. Notably, the rate constant for the chair-boat conformation interconversion exhibited a linear correlation with applied pressure. Furthermore, high-pressure neutron powder diffraction studies on piperidine have demonstrated significant pressure-induced deformation of its crystal structure within the pressure range of 0.22–2.77 GPa [19]. These studies indicated that van der Waals interactions primarily drive the quasi-isotropic volume contraction observed in the crystal. Complementary investigations into the structure of 1-methylpiperidine hydrogen clathrate hydrates have confirmed that the synergistic effects of high pressure and the size of auxiliary guest molecules can influence phase stability by regulating the

* Corresponding author.
** Corresponding author at: Zhengzhou University of Light Industry, Zhengzhou, Henan, 450002, China.
*E-mail addresses:* zzyuancs@zzuli.edu.cn (C. Yuan), lei.su@sharps.ac.cn (L. Su).

https://doi.org/10.1016/j.cplett.2026.142796
Received 6 January 2026; Received in revised form 28 March 2026; Accepted 31 March 2026
Available online 1 April 2026

strength of hydrogen bonding interactions [20].

However, despite some studies implying the high-pressure response characteristics of 1-methylpiperidine, a systematic investigation into the high-pressure phase transitions of its bulk form remains largely unexplored. Specifically, there is a conspicuous absence of research that systematically elucidates the influence of kinetic factors, such as pressure loading rate, pressure holding time, and cooling/heating rates, on these phase transition processes. To address this knowledge gap, we selected 1-methylpiperidine as our model compound and designed and executed a series of high-pressure experiments. These experiments utilized diamond anvil cell (DAC) technology for generating high pressures, coupled with in-situ Raman spectroscopy for characterization. Our primary objective was to systematically investigate the evolution of the crystal structure of 1-methylpiperidine across a pressure range of 0–21 GPa.

## 2. Experimental methods

All experiments were conducted using a Merrill-Bassett four-screw diamond anvil cell (DAC) equipped with two diamonds, each with a 300 μm culet size. To serve as the sample chamber, a hole with a diameter of 80 μm was drilled at the center of a 300 μm thick T301 gasket that had been pre-indented to a thickness of 100 μm. This central hole in the DAC gasket was then filled with 99.59800 wt% 1-methylpiperidine liquid, sourced from Shanghai Aladdin Pharmaceutical Co., Ltd., along with a small ruby chip. Following this, the gasket was hermetically sealed using the opposing anvil. The chamber pressure was calibrated by using the ruby *R1* fluorescence line [21].

Two experiments (static and dynamic compression) were conducted when 1-methylpiperidine was subjected to extreme conditions. A standard four-screw diamond anvil cell (DAC) was used for static compression experiments, in which the sample was steadied and gradually compressed before Raman spectra were gathered. Dynamic compression experiments were conducted on the d-DAC, which is constituted by a metal frame, a piezoelectric (PE) actuator, a control system, and a standard DAC. The PE actuator (Harbin Core Tomorrow Science & Technology Co., Ltd.) was assembled on the top of the metal frame. A conventional DAC was fixed at the bottom of the metal frame by a steel plate and a static load screw. The pressure control system can be configured to provide an output voltage within the range of 0 to 120 *V*, and this device can achieve a pressure jump within 5 ms [22]. In this work, all compression and decompression experiments were performed by directly loading the liquid sample between the diamond anvils of a DAC. Since 1-methylpiperidine remains highly fluid under low-pressure conditions, it can effectively alleviate shear stress and ensure good hydrostatic conditions and pressure uniformity within the sample chamber. Therefore, no pressure-transmitting medium was used during the experiments.

Raman spectroscopy experiment were performed utilizing a Renishaw inVia Raman microscope (Renishaw, UK) with an excitation wavelength of 532 nm. Spectral data were acquired in a backscattering configuration, employing a 2400 g/mm holographic grating, and the slit width was selected as 65 μm, which corresponded to a resolution of approximately 0.5 $cm^{-1}$. Sample imaging was achieved via an achromatic lens integrated into the optical microscope, with the image subsequently focused onto a charge-coupled device (CCD) detector to enable visual monitoring throughout the experimental process. The obtained Raman spectra were fitted with a mixed Gaussian-Lorentzian function using WIRE 3.3 software (Renishaw, United Kingdom) to analyze the spectral data.

Notably, during the three static compression experiments, constant ambient temperature, uniform experimental duration, consistent sample preparation, and unchanged Raman spectrometer parameters were adopted to ensure the comparability of spectral data. The sample was stabilized after static compression before spectrum collection. All samples were purchased from Aladdin Industrial Corporation with identical purity and loading method. The parameters of the Raman spectrometer, including laser power, integration time and wavenumber range, remained constant throughout all measurements.

## 3. Results and discussion

### 3.1. Static compression experiments: Kinetically controlled polymorphism and amorphization

#### 3.1.1. Run 1 (21.50 GPa): Phase I (1.54 GPa) → phase II (1.32 GPa) → amorphization

Fig. 1 illustrates the Raman spectrum of 1-methylpiperidine acquired under static compression up to 21.50 GPa at ambient temperature. The Raman peak assignments of 1-methylpiperidine are summarized in Table 1. Generally, the characteristic vibrational modes exhibited a blueshift (movement to higher wavenumbers) as pressure increased. This blue-shifting behavior is directly attributable to the pressure-induced shortening of intermolecular distances. However, a crucial sign of a structural rearrangement was the appearance of spectral anomalies at 1.54 GPa. In the low-frequency range of 50–150 $cm^{-1}$, additional raman peaks that corresponded to lattice vibrational modes appeared. Significant spectrum evolution took place in the internal vibrational domains (1400–1500 $cm^{-1}$ and 2850–3000 $cm^{-1}$) at the same time. At this critical pressure, the presence of two distinct peaks (at 369 and 809 $cm^{-1}$) and significant splitting (i.e., the conversion of the 1037 $cm^{-1}$ peak into sharp components at 1033 and 1044 $cm^{-1}$ and the 1138 $cm^{-1}$ peak into 1139 and 1145 $cm^{-1}$) clearly suggests a liquid-to-crystalline transition (Phase I).

To evaluate the thermodynamic stability of the crystalline structures, Phase I of 1-methylpiperidine, synthesized at 1.54 GPa, was subjected to an isobaric hold for 1 h at room temperature. Intriguingly, this isobaric hold period resulted in an unintentional pressure relaxation within the sample chamber, dropping the pressure to 1.32 GPa. This decompression is further accompanied by changes in the Raman spectrum, indicating the destabilization or transformation of the initial phase I. At 1.32 GPa, the Raman spectra displayed marked variations compared to the 1.54 GPa state, particularly evident in the lattice modes (50–200 $cm^{-1}$) and key molecular fingerprints (1400–1500 $cm^{-1}$ and 2850–3000 $cm^{-1}$). The spectral evolution upon this pressure drop included: the disappearance of the 809 $cm^{-1}$ mode and the sharpening of the 556 $cm^{-1}$ peak; the fission of the 868 $cm^{-1}$ peak into distinct components at 855 and 865 $cm^{-1}$ (suggesting symmetry reduction); and the merging and collapse of several bands, such as the transformation of the 1033 and 1043 $cm^{-1}$ doublet into a single sharp peak at 1039 $cm^{-1}$. These changes indicate that 1-methylpiperidine forms as a new high-pressure phase (Phase II) at 1.32 GPa. The structural transition suggests that the phase I at 1.54 GPa is kinetically or thermodynamically unstable and spontaneously transforms into the stable Phase II. This kinetic dependence on the pressure history highlights the metastable phase behavior of 1-methylpiperidine under High Pressure. It should be clarified that the division of Phase I, Phase II, and Phase III in this study is based on the reproducible Raman spectral characteristics observed during the static compression process.

A predicted property of compression, the lattice stiffening, was seen as pressure was progressively increased: all Raman characteristics showed a positive pressure shift (blueshift). Crucially, throughout the observed range, no new vibrational modes nor extinguished modes were detected. This spectral feature clearly shows that Phase II preserves thermodynamic and structural integrity during the continual compression process. However, when the pressure exceeds 10.93 GPa, all Raman characteristic peaks exhibit significant broadening, reduced intensity, and gradually become indistinguishable. Such behavior is indicative of pronounced structural disorder and severe lattice distortion under high pressure, which may originate from crystal fragmentation and the loss of long-range order.

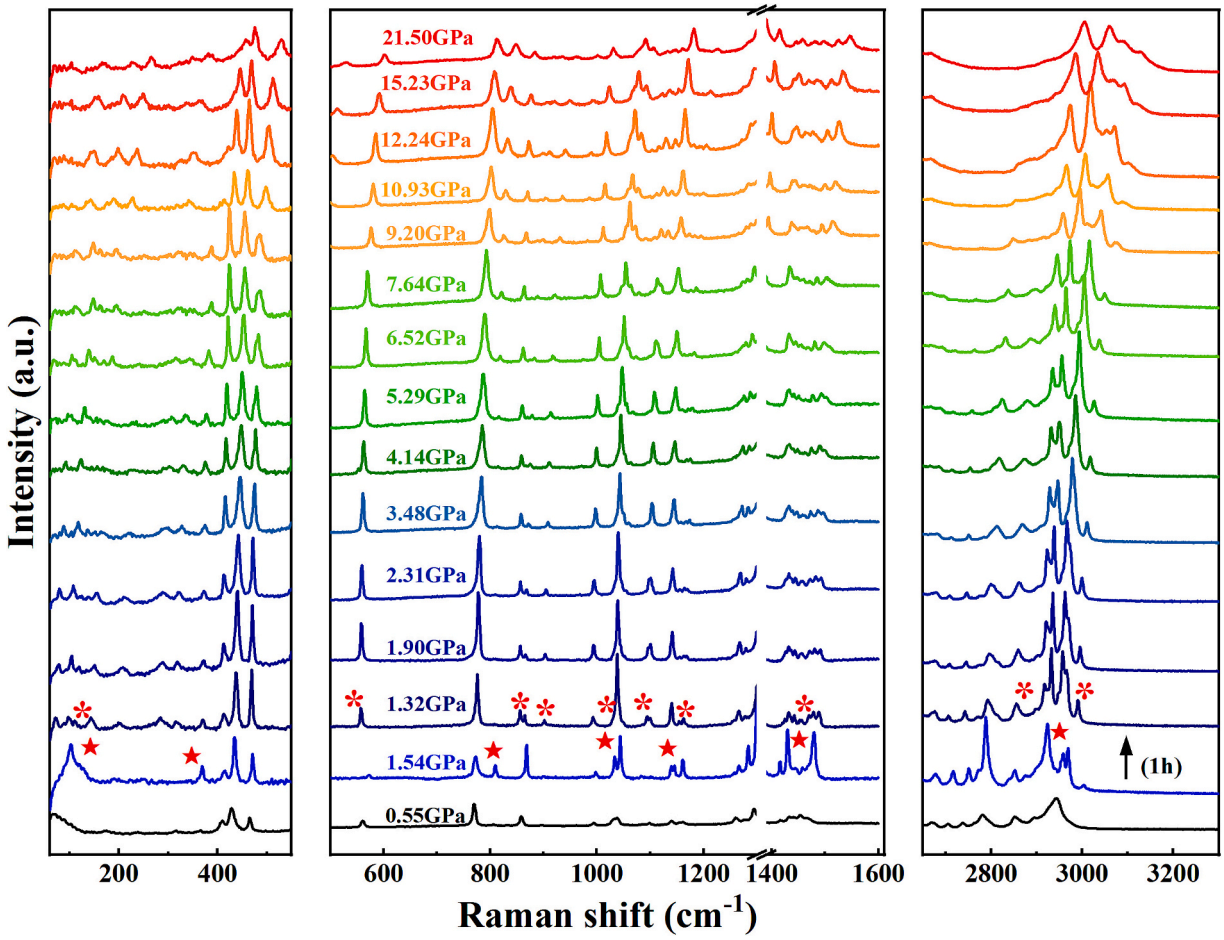


**Fig. 1.** Raman spectra of 1-methylpiperidine in Static Compression Run 1 (up to 21.50 GPa); The asterisks (★) denote the characteristic Raman peaks of 1-methylpiperidine at 1.54 GPa, and the asterisks (*) represent those at 1.32 GPa. The arrow (↑) indicates that the pressure on 1-methylpiperidine was relaxed from 1.54 GPa to 1.32 GPa after holding for 1 h.

**Table 1**
Raman peak assignments of 1-methylpiperidine.

| Raman shift($cm^{-1}$) | Vibrational assignment [30] |
|---|---|
| 371 | Ring skeletal vibration |
| 432 | Ring skeletal vibration |
| 570 | Ring skeletal vibration |
| 827 | $CH_2$ bending vibration: Rocking |
| 860 | Ring skeletal vibration |
| 937 | $CH_2$ bending vibration: Rocking |
| 1145 | $CH_2$ bending vibration: Twisting |
| 1170 | $CH_2$ bending vibration: Twisting |
| 1291 | $CH_2$ bending vibration: Wagging |
| 1436 | H–C–H bending vibration: Scissoring/in-plane bending |
| 1471 | H–C–H bending vibration: Scissoring/in-plane bending |
| 2665 | C–H stretching vibration |
| 2739 | C–H stretching vibration |
| 2777 | C–H stretching vibration |
| 2841 | C–H stretching vibration |

*3.1.2. Run 2 (20.06 GPa): Over-pressurized liquid → phase III (2.15 GPa) → amorphization*

To investigate the reproducibility of the previously reported metastable phase transition in 1-methylpiperidine, two independent static compression experiments were conducted at room temperature. Critically, the results of these verification runs diverged significantly from the initial observations. In the first repetition, the sample remained in the liquid phase even when compressed up to 2.17 GPa, suggesting the formation of an over-pressurized liquid. However, post-isobaric holding for 1 h at 2.17 GPa, optical microscopy revealed the nucleation of minute crystalline clusters, accompanied by an abrupt, spontaneous pressure decrease to the transformation pressure of 2.15 GPa. Fig. 2 illustrates the Raman spectral evolution under static compression. At the initial pressurization endpoint of 2.17 GPa, the spectrum closely mirrored that of the liquid phase reported at 0.58 GPa. Following the 1 h isobaric hold, the system underwent the characteristic liquid-to-solid transition (Phase III) at 2.15 GPa, evidenced by definitive spectroscopic changes. The appearance of new lattice vibration modes in the 50–200 $cm^{-1}$ range, confirming the onset of long-range order; Significant mode splitting, such as the transformation of the peak at 471 $cm^{-1}$ into 466 $cm^{-1}$ and 480 $cm^{-1}$, and the resolution of the 1042 $cm^{-1}$ band into 1027 $cm^{-1}$ and 1044 $cm^{-1}$. Furthermore, the high frequency modes, the C—H stretching region showed that the peak at 2954 $cm^{-1}$ decomposed into five distinct sharp peaks (2924, 2942, 2959, 2965, and 2974 $cm^{-1}$). These pronounced spectral features confirm that Phase III formation in this instance resulted from the spontaneous crystallization of the over-pressurized liquid phase during the isobaric hold process at 2.15 GPa. With further increasing pressure, the Raman peaks of phase III show no significant changes; until the pressure exceeds 10.53 GPa, the Raman peaks gradually broaden with reduced intensity, indicating the system undergoes an amorphization process.

*3.1.3. Run 3 (21.50 GPa): Amorphous phase formation at low pressure (2.0 GPa) and its stability*

In the second repetition, 1-methylpiperidine was slowly compressed to 2.0 GPa, with 1 h of isobaric holding. Throughout the process, the

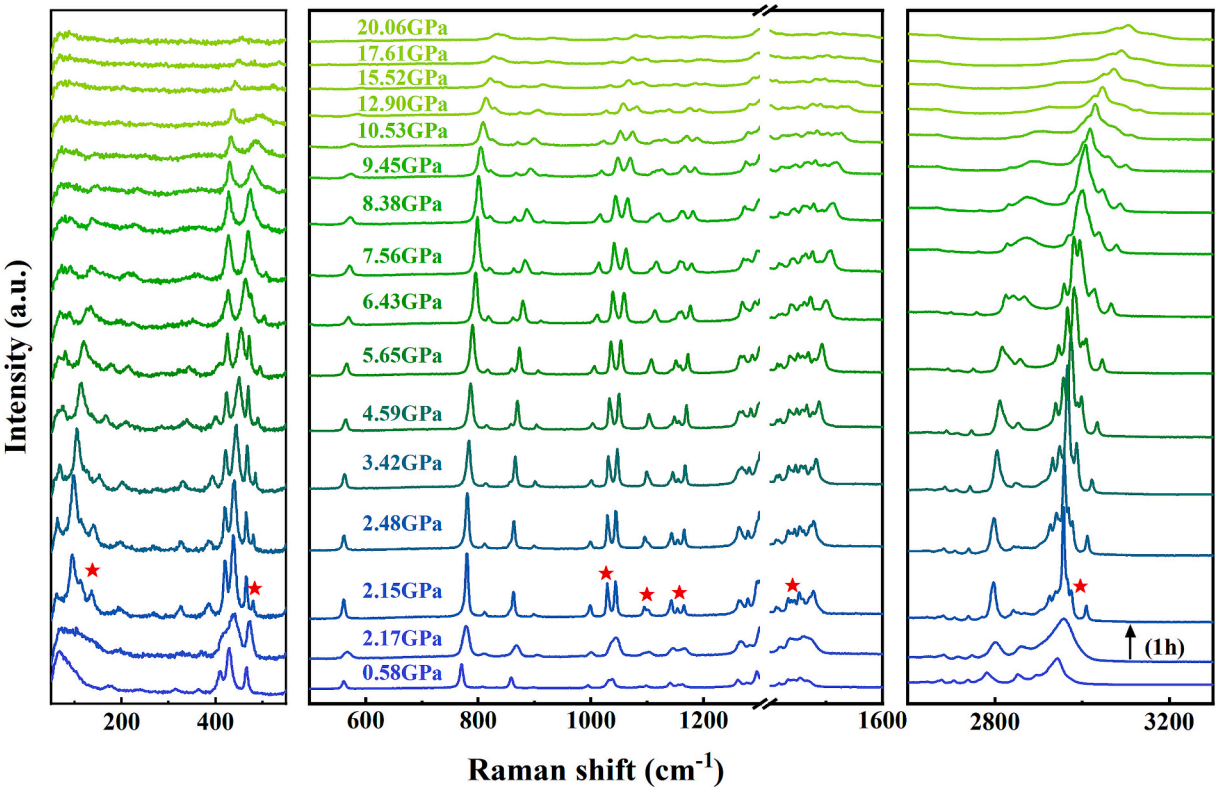


**Fig. 2.** Raman spectra of 1-methylpiperidine in Static Compression Run 2 (up to 20.06 GPa); The asterisks (★) denote the characteristic Raman peaks of 1-methylpiperidine at 2.15 GPa. The arrow (↑) indicates that the pressure on 1-methylpiperidine was relaxed from 2.17 GPa to 2.15 GPa after holding for 1 h.

sample chamber remained transparent, with no fine crystals or distinct phase boundaries observed. Fig. 3 shows the Raman spectrum of 1-methylpiperidine under static compression. It can be seen that, the Raman peaks of the sample kept isobarically at 2 GPa for 1 h do not significantly differ from those of the liquid sample, and no discernible lattice vibration peaks are seen in the 50–400 $cm^{-1}$ region. In contrast to the previously reported crystalline transitions (or crystallization events) at 1.57 GPa and 2.15 GPa, it appears that an amorphous phase of 1-methylpiperidine is generated at a pressure of 2.0 GPa. Additional isobaric holding experiments were carried out at 2.5 GPa and 2.8 GPa to define the upper pressure limit for the stability of the amorphous phase; both tests verified that the amorphous phase remained stable. Upon further compression, the Raman peaks in 1-methylpiperidine gradually become smooth or indistinct. This observation can be ascribed to the pressure-

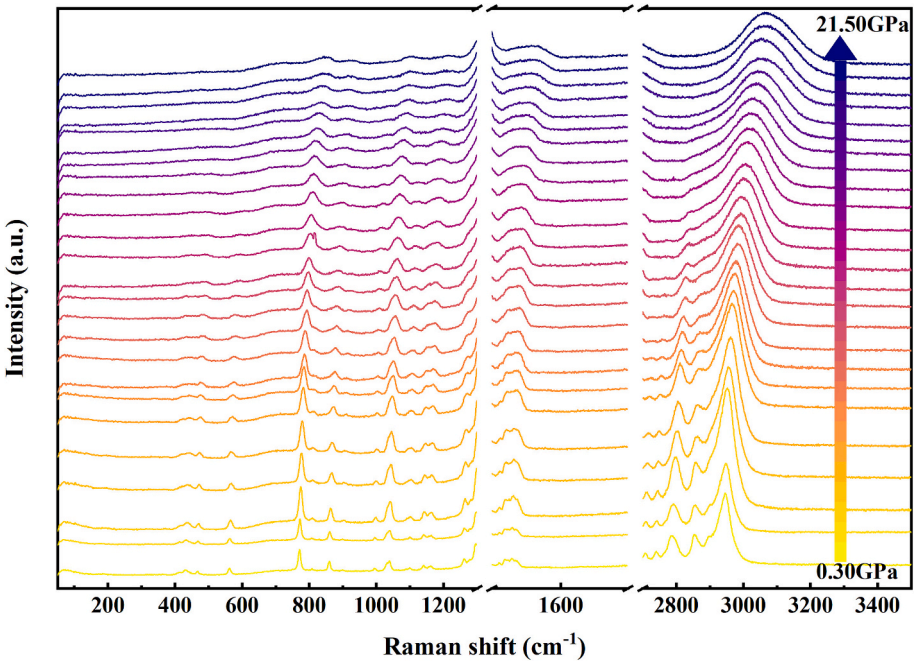


**Fig. 3.** Raman spectra of 1-methylpiperidine in Static Compression Run 3 (up to 21.50 GPa).

induced acceleration of intramolecular dynamics, which consequently induces a dynamic averaging of the Raman spectral responses.

Run 1, Run 2, and Run 3 were subjected to decompression, and all samples exhibited reversible behavior during the decompression process. In addition, crystallization occurred during the decompression of Run 3, with a transformation from the amorphous phase to a crystalline phase II. The decompression spectra of the three runs are presented in **Fig. S1** in the Supporting Information. The experimental results demonstrate that 1-methylpiperidine exhibits polymorphism under slow compression and solidification, yielding four distinct solid phases (Phase I, Phase II, Phase III, and an amorphous phase). Fig. 4 presents a comparative analysis of the Raman spectra for these four phases. While the vibrational mode differences between Phase I and Phase II have been elaborated in prior sections, Phase III displays spectral characteristics that suggest a relationship with both. Specifically, complementary peaks, namely those at 809, 862, 1021, and 1044 $cm^{-1}$, are common to both Phase I and Phase III. Concurrently, peaks at 558, 901, 1094, and 1100 $cm^{-1}$ are observed in both Phase II and Phase III. Based on this shared spectral signature, it is postulated that Phase III may represent a composite or co-existing mixture of Phase I and Phase II.

As mentioned above, the complex polymorphism exhibited by 1-methylpiperidine during three cycles of slow compression and solidification, encompassing the observation of phases I, II, III, and an amorphous state, is driven by pressure-induced structural transformations and energy landscape regulation. Since the chair and boat conformations of the piperidine ring may coexist, 1-methylpiperidine molecules have inherent structural flexibility that permits a variety of spatial configurations and stacking orientations in the solid state. These different molecular packing configurations match several possible system energy minima. Thus, the system can "explore" these metastable energy minima and eventually arrive at thermodynamically stable states through the gradual compression and solidification process.

At 1.54 GPa, the system evolves primarily through nucleation and growth kinetics, with molecular structure fixed in the comparatively higher-energy Phase I. And then, the system experiences spontaneous rearrangement motivated by energy reduction throughout the next 1-h isothermal holding phase. More efficient packing and stacking arrangements are adopted by molecules, which facilitates transition to the lower-energy phase II. In addition, 1-methylpiperidine solidifies into an "overpressurized liquid" and an "amorphous state" when gradually compressed to 2.17 GPa and 2.0 GPa, respectively. The formation of non-crystalline states during gradual compression is due to kinetic trapping from hindered molecular rearrangement/nucleation (not insufficient time). This over-pressurized liquid may concurrently transition to phases I and II in response to minute changes in temperature or volume. The emergence of the mixed state constructs a new energy barrier, which hinders the transformation from Phase I to Phase II and ultimately facilitates the formation of the ordered mixed Phase III. In addition, Furthermore, the amorphous form benefits from greatly increased intermolecular interactions at high pressure, which deepens the potential well depth and, as a result, improves stability in this high-pressure setting.

In summary, the polymorphic evolution of 1-methylpiperidine is a result of the synergistic interplay between pressure-driven thermodynamic evolution, the inherent conformational flexibility of the molecule, the limitations of crystallization kinetics, and the resultant formation mechanisms of mixed phases. Notably, the amorphous state acquires significantly enhanced stability at high pressures due to the strengthening of intermolecular interactions.

### 3.2. *Dynamic compression experiments: Rapid amorphization at ~$10^3$ GPa/s*

In the dynamic compression experiment, 1-methylpiperidine was first slowly compressed to 1.04 GPa at room temperature (where the sample remained in the liquid state), and then rapidly pressurized to 11.41 GPa within 5 ms. Fig. 5 shows the comparison of the Raman spectra of 1-methylpiperidine before and after this process. At 1.04 GPa, the sample's Raman spectra shows a number of distinct, crisp, and resolvable peaks in the 200–1600 $cm^{-1}$ region, including peaks at about 800 and 1200 $cm^{-1}$. Multiple abrupt C—H stretching peaks (e.g., at ~3000 $cm^{-1}$) are seen in the 2800–3400 $cm^{-1}$ range. For the sample at

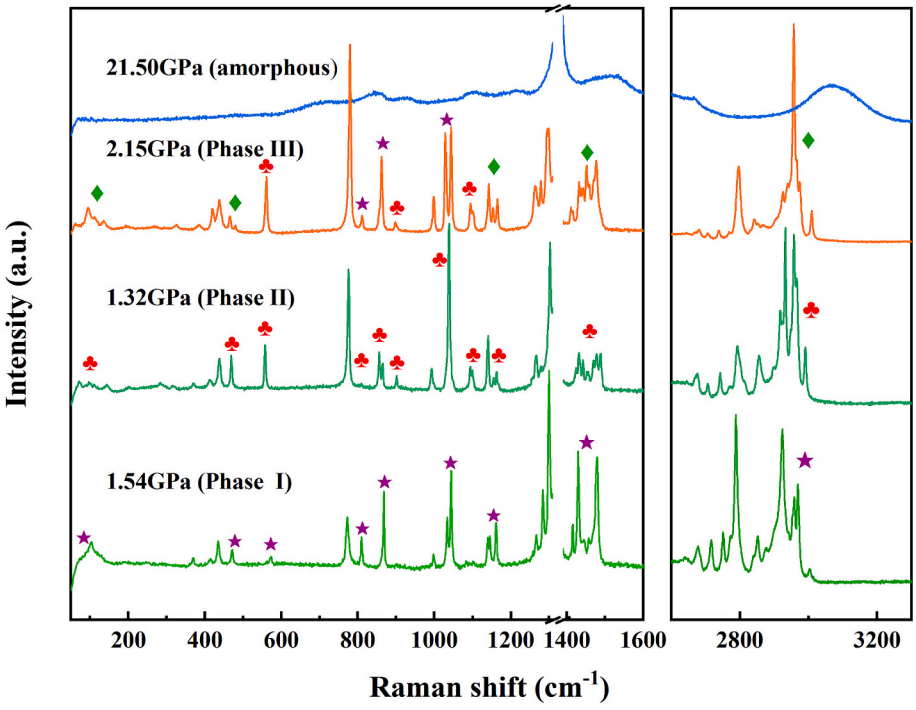


**Fig. 4.** The Raman spectra of the three crystal forms of 1-methylpiperidine; Asterisks (★) represent the characteristic peaks of Phase I, plum blossom symbols (♣) represent those of Phase II, and diamond symbols (◆) represent those of Phase III.

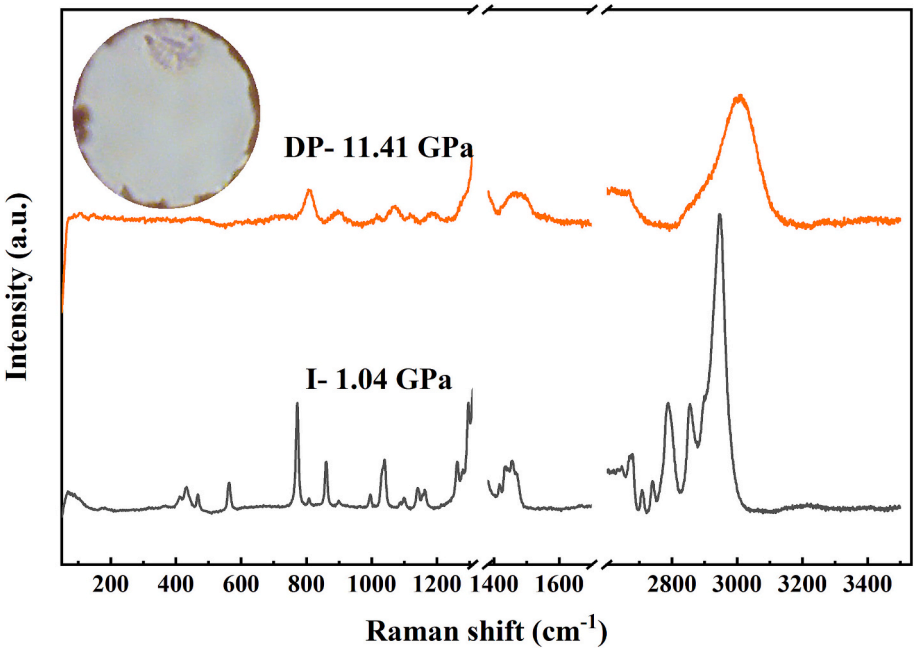


**Fig. 5.** Raman spectra of 1-methylpiperidine in Dynamic Compression (1.04 GPa → 11.41 GPa); The inset shows photograph of the sample at 11.41 GPa. "DP-" represents dynamic compression; "I-" represents initial pressure.

DP-11.41 GPa, most characteristic peaks in the 200–1600 $cm^{-1}$ range broaden, shift, or disappear, leaving only a few broadened peak envelopes. Concurrently, the C—H stretching peaks in the 2800–3400 $cm^{-1}$ range transform into broadened envelopes. This phenomenon arises from significantly enhanced intermolecular interactions (e.g., van der Waals forces and dipole-dipole interactions) under high pressure, which lead to a significant increase in the long-range disorder of molecular packing and considerably restrict the vibrational flexibility of the methyl groups. Following pressurization, the sample appears uniformly amorphous in the optical micrograph, without any crystallographic characteristics like facet reflections or grain boundaries. The Raman spectra's peak widening and disappearance, which together validate the amorphous phase of 1-methylpiperidine under dynamic compression.

### *3.3. Decompression experiments: Spontaneous crystallization of amorphous phase*

The stability of the amorphous 1-methylpiperidine formed under dynamic pressure was subsequently investigated using Raman spectroscopy throughout a gradual pressure release. The decompression Raman spectra and accompanying images of 1-methylpiperidine (DP-11.41 GPa) during this procedure are shown in Fig. 6. All of the Raman peaks first displayed a redshift when the pressure was lowered to 2.26 GPa (Fig. 6(a)); crucially, however, neither new peaks nor old peaks vanished. This conduct attests to the amorphous phase's ongoing structural integrity. However, when the pressure was further reduced to 2.17 GPa, a notable shift was noted. In particular, the lattice vibration area showed distinct, sharp peaks, such as those at 421, 439, 466, and 560 $cm^{-1}$. These spectroscopic signals unequivocally show that during the pressure release from 11.41 GPa to 2.17 GPa, 1-methylpiperidine underwent a phase change from amorphous to crystalline. There are also two strong peaks at 1028 $cm^{-1}$ and 1043 $cm^{-1}$, a sharp peak at 860 $cm^{-1}$, weak peaks at 1095 $cm^{-1}$ and 1101 $cm^{-1}$, and additional weak peaks at 480 $cm^{-1}$ and 900 $cm^{-1}$. Fig. 3 shows that these Raman spectral peaks correspond to Phase III during the static compression process. Thus, 1-methylpiperidine is thought to change into the crystalline Phase III upon release to 2.17 GPa. Additional spectral changes took place as the pressure dropped to 1.65 GPa: the sharp peak at 862 $cm^{-1}$ split into two peaks at 857 $cm^{-1}$ and 865 $cm^{-1}$, the weak peak at 480 $cm^{-1}$ disappeared, and the two sharp peaks at 1028 $cm^{-1}$ and 1043 $cm^{-1}$ changed into a sharp peak at 1039 $cm^{-1}$ and a weak peak at 1029 $cm^{-1}$. These changes align with Phase II, which is seen when compression is static. Therefore, it can be concluded that when pressure is reduced to 1.65 GPa, 1-methylpiperidine changes from crystalline Phase III to Phase II. All of the Raman peaks expanded considerably with further release to 1.02 GPa, and the lattice vibration area lost all peaks, resembling the original spectrum at atmospheric pressure. This suggests that the initial liquid state may have been reverted below 1.02 GPa.

Photographic proof of the 1-methylpiperidine crystallization process during decompression is also shown in **Fig. 6(b)** and **(c)**. As seen in Fig. 6(b), a tiny number of crystals started to nucleate near the cavity's border as soon as the material was released to 2.17 GPa. The cavity filled with crystals during a ten-minute hold at this pressure. This whole crystal formation was noteworthy since it happened on its own. Subsequently, the big crystals that were already present in the cavity became smaller and finer when the pressure was lowered below 1.65 GPa. Fig. 6 (c) shows that the crystals melted back into the original liquid condition after additional decompression to 1.02 GPa. Based on these results, 1-methylpiperidine experiences three phase transitions during pressure release from 11.41 GPa: amorphous-to-crystalline at 2.17 GPa, crystal-to-crystal at 1.65 GPa, and crystal-to-liquid at 1.02 GPa.

### *3.4. Influence of compression rate: Comparison between static and dynamic results*

As mentioned above, 1-methylpiperidine exhibits complex phase behavior under high pressure, where the compression rate significantly influences its crystallization pathway. Under slow static compression, molecules have ample time to explore the energy landscape and overcome kinetic barriers [23–25], leading to the formation of polymorphs (Phase I, II, III) as well as metastable superpressurized liquid and amorphous states. The evolution of these phases, particularly the considerable variability in repeated experiments, underscores the critical role of kinetic limitations, nucleation processes, and intramolecular conformational flexibility (coexistence of chair and boat conformers) in dictating high-pressure structures. For instance, the formation of Phase

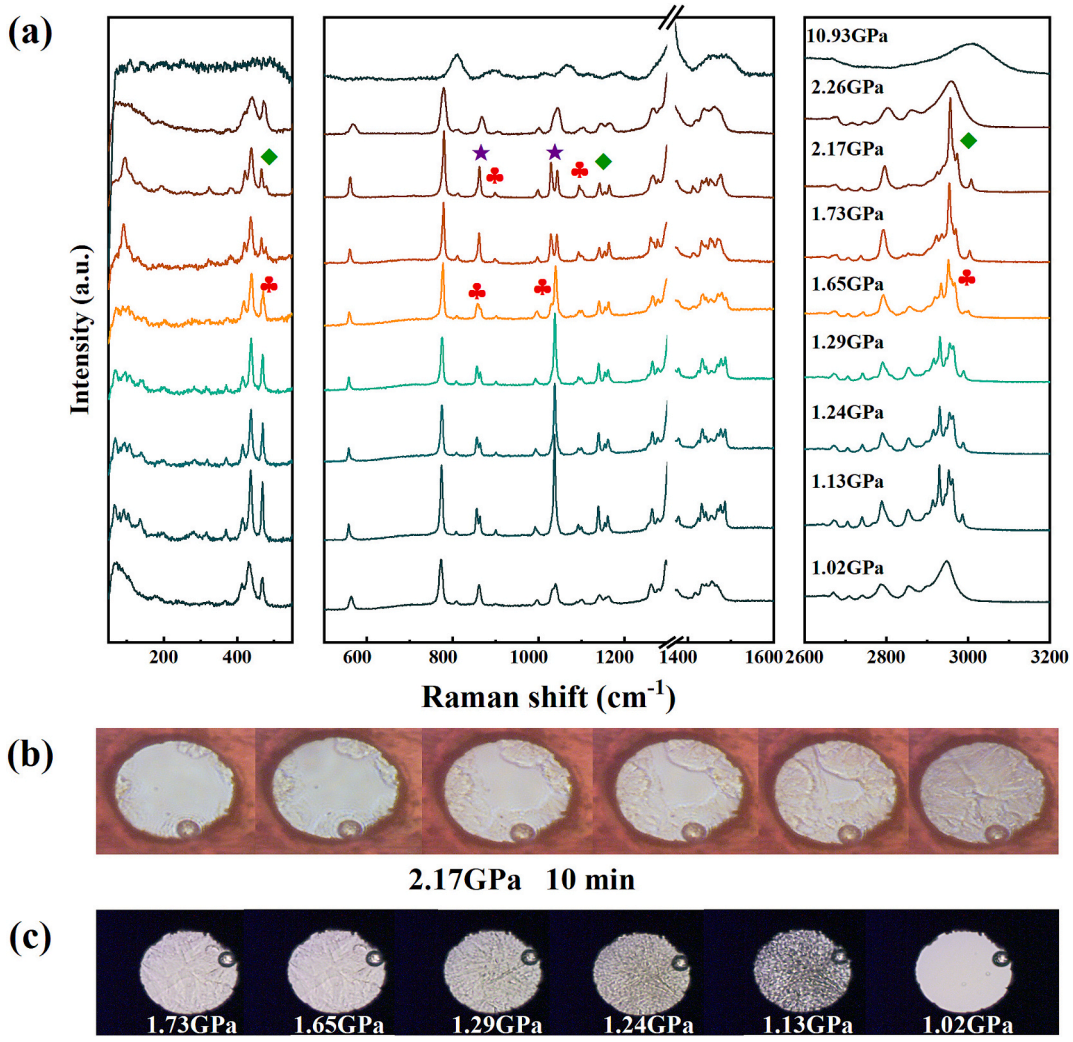


**Fig. 6.** (a) Raman spectra and optical images of 1-methylpiperidine in Decompression after Dynamic Compression; Asterisks (★) represent the characteristic peaks of Phase I, plum blossom symbols (♣) represent those of Phase II, and diamond symbols (◆)) represent those of Phase III. (b) Photograph of 1-methylpiperidine crystallization process by decompression at 2.17 GPa. (c) Photograph of the crystal melting process of 1-methylpiperidine at 1.73 GPa.

III is proposed to be a mixed phase, reflecting the molecule's intricate exploration of its energetic minima [26]. To intuitively illustrate the kinetically controlled polymorph formation mechanism, a schematic potential energy landscape (PEL) of 1-methylpiperidine at different pressure regimes is presented in **Fig. S2**. At low pressure (<2 GPa), the PEL exhibits multiple shallow energy minima with small, closely spaced kinetic barriers, corresponding to the liquid, Phase I, Phase II and Phase III. This characteristic enables the system to be trapped in different metastable states depending on nucleation kinetics and isobaric holding time, resulting in the diverse phase behavior observed in static compression runs. At medium pressure (2–10 GPa), Phase II becomes the thermodynamically most stable state with a deeper energy minimum, and the increased kinetic barriers ensure the structural stability of crystalline phases. At high pressure (>10 GPa), the crystal lattice is broken by mechanical stress, leading to the elevation of crystalline phase energy minima and the formation of a deep energy minimum for the amorphous state. For static compression, the system overcomes the low kinetic barrier from crystalline phases to the amorphous state (mechanical amorphization); for dynamic compression, the rapid compression rate quenches molecular rearrangement, leading the system to be directly trapped in the amorphous state without crystalline phase formation [27,28]. During decompression, the amorphous state crosses low kinetic barriers to sequentially enter the Phase III and Phase II minima, consistent with the spontaneous crystallization behavior observed in our experiments. Further demonstrating the profound impact of kinetic history on attainable phases [29]. Therefore, the polymorphic behavior of 1-methylpiperidine under high pressure is a kinetically sensitive process rather than a purely thermodynamic equilibrium transformation.

## 4. Conclusions

This study systematically explored the pressure-induced phase behavior of 1-methylpiperidine under static and dynamic compression, revealing a kinetically sensitive, complex polymorphic landscape. Under slow static compression, multiple crystalline phases (I, II, and III), as well as metastable over-pressurized liquid and amorphous states, were observed. The transformation pathways depended heavily on pressure history, holding time, and kinetic accessibility to energy minima. Notably, Phase III appeared to be a mixture of Phases I and II, indicating intricate molecular packing and interaction effects. Variations between experiments highlight that nucleation and growth kinetics dominate the phase outcome over thermodynamic control. Conversely, rapid dynamic compression suppressed molecular rearrangements, producing a disordered amorphous phase directly. During decompression, this amorphous state spontaneously crystallized through Phases III and II before reverting to liquid at lower pressure, emphasizing the critical role of compression rate. Overall, these results show that the high-pressure

phase diagram of 1-methylpiperidine is governed by kinetic factors and molecular flexibility, which enable the exploration of a complex energy landscape with kinetically trapped metastable states. The amplification of intermolecular interactions at high pressure stabilizes both polymorphs and amorphous phases, offering valuable insights into the pressure-driven structural evolution of organic molecules and underscoring the importance of kinetic considerations in condensed matter physics.

## CRediT authorship contribution statement

**Qingqing Yang:** Writing – original draft, Software, Methodology, Investigation, Data curation, Conceptualization. **Chaosheng Yuan:** Writing – review & editing, Writing – original draft, Supervision, Methodology, Investigation, Funding acquisition, Data curation, Conceptualization. **Chenran Zhang:** Validation, Resources, Methodology, Funding acquisition. **Xuerui Cheng:** Visualization, Supervision, Formal analysis, Conceptualization. **Haining Li:** Software, Project administration, Methodology. **Yongfu Liang:** Visualization, Software, Resources. **Zheng Wang:** Resources, Project administration, Methodology. **Xiang Zhu:** Software, Resources, Investigation. **Lei Su:** Writing – review & editing, Supervision, Methodology, Investigation, Funding acquisition.

## Declaration of competing interest

The authors declare that they have no known competing financial interests or personal relationships that could have appeared to influence the work reported in this paper.

## Acknowledgments

This work is supported by the National Science Foundation of China (No.21503194; No.12104415); the Scientific Research Key Project Foundation of Henan Province (No.242102230109; No.252102241031); Natural Science Foundation of Henan Province (No.252300420354; No.262300420345).

## Appendix A. Supplementary data

Supplementary data to this article can be found online at https://doi.org/10.1016/j.cplett.2026.142796.

## Data availability

Data will be made available on request.

## References

[1] M. Wojcieszak, A. Syguda, A. Lewandowska, et al., Synthesis and surface properties of Piperidinium-based herbicidal ionic liquids as a potential tool for weed control, J. Agric. Food Chem. 71 (11) (2023) 4550–4560, https://doi.org/10.1021/acs.jafc.3c00356.
[2] V.M. Pulga, J. Harp, T.E. Reeves, Molecular modeling and potential ca2+ channel blocker activity of diphenylmethoxypiperidine derivatives, Chemistry 5 (2) (2023) 713–719, https://doi.org/10.3390/chemistry5020050.
[3] C. Holtschulte, F. Börgel, S. Westphälinger, et al., Synthesis of aminoethyl-substituted piperidine derivatives as σ1 receptor ligands with antiproliferative properties, ChemMedChem 17 (7) (2022) e202100735, https://doi.org/10.1002/cmdc.202100735.
[4] M.A.V. Ribeiro da Silva, J.I.T.A. Cabral, P. Gomes, et al., Combined experimental and computational study of the thermochemistry of methylpiperidines, J. Org. Chem. 71 (10) (2006) 3677–3685, https://doi.org/10.1021/jo052468w.
[5] A.R. Katritzky, R.C. Patel, F.G. Riddell, N-methyl inversion barriers in six-membered rings, Angew. Chem. Int. Ed. Engl. 20 (1981) 521–529, https://doi.org/10.1002/anie.198105211.
[6] M.T. Güllüoğlu, Y. Erdoğdu, Ş. Yurdakul, Molecular structure and vibrational spectra of piperidine and 4-methylpiperidine by density functional theory and ab initio Hartree-Fock calculations, J. Mol. Struct. 834-836 (2007) 540–547, https://doi.org/10.1016/j.molstruc.2007.01.023.
[7] T. Hirokawa, T. Kimura, K. Ohno, Vibrational spectra of piperidine, pyrrolidine, morpholine, and their n-methyl derivatives adsorbed on aerosil silica, Spectrochim. Acta A 36 (3) (1980) 329–332, https://doi.org/10.1016/0584-8539(80)80138-3.
[8] G. Marcotrigiano, L. Menabue, G.C. Pellacani, Infrared sprctea (4000-60 $cm^{-1}$) of the antimony(III) and bismuth(III) trihalide complexes with piperidine and piperidine, J. Mol. Struct. 30 (1) (1967) 85–94, https://doi.org/10.1016/0022-2860(76)85048-X.
[9] Y. Okishi, Y. Imai, K. Aida, NH stretching frequencies and the structures of i2 and IBr complexes with piperidine and piperazine, J. Inorg. Nucl. Chem. 35 (1) (1973) 101–107, https://doi.org/10.1016/0022-1902(73)80615-3.
[10] I.-G. Grosu, A. Turza, G. Borodi, et al. The crystal structures of 4-(1-Methylpiperidin-1-ium-1-yl)-2,2-Diphenylbutanamide bromide and 4-(1-Methylpiperidin-1-ium-1-yl)-2,2-Diphenylbutanamide bromide hemihydrate. Molbank 2024, 2024(4), M1904. doi:https://doi.org/10.3390/M1904.
[11] H.T. Zhao, Modulating conformational preferences by allylic strain toward improved physical properties and binding interactions, ACS Omega 7 (10) (2022) 9080–9085, https://doi.org/10.1021/acsomega.2c00510.
[12] M.R. Ward, C.L. Bull, N.P. Funnell, Exploring the effects of high pressure on hydrogen bonding in pharmaceutical cocrystals: a systematic study of pyridine dicarboxylic acid systems using synchrotron and neutron diffraction, Int. J. Pharm. 647 (25) (2023) 123514, https://doi.org/10.1016/j.ijpharm.2023.123514.
[13] Richard H. Jones, Craig L. Bull, Kevin S. Knight, et al., High-pressure induced switching between halogen and hydrogen bonding regimes in 1,4-dioxane iodine monochloride, CrystEngComm 25 (2023) 4146–4156, https://doi.org/10.1039/D3CE00362K.
[14] P. Pruzan, Pressure effects on the hydrogen bond in ice up to 80 GPa, J. Mol. Struct. 322 (1994) 279–286, https://doi.org/10.1016/0022-2860(94)87045-4.
[15] X.D. Wen, R. Hoffmann, N.W Ashcroft, Benzene under high pressure: a story of molecular crystals transforming to saturated networks, with a possible intermediate metallic phase. J. Am. Chem. Soc. 2011, 133 (23) 9023–9035. doi: https://doi.org/10.1021/ja201786y.
[16] H. Wang, X. Li, G. Gao, et al., Hydrogen-rich superconductors at high pressures, WIREs Comput. Mol. Sci. 2018,8 (1) e1330. doi:https://doi.org/10.1002/wcms.1330.
[17] Z. Gan, Y. Liu, L. Wang, et al., Distance makes a difference in crystalline photoluminescence, Nat. Commun. 11 (1) (2020) 5572, https://doi.org/10.1038/s41467-020-19377-6.
[18] M. Tafazzoli, C. Suarez, N.S. True, et al., Pressure-and temperature-dependent proton NMR studies of n-methylpiperidine ring inversion in the gas phase, J. Phys. Chem. 96 (25) (1992) 10201–10205, https://doi.org/10.1021/j100204a021.
[19] L.E. Budd, R.M. Ibberson, W.G. Marshall, et al., The effect of temperature and pressure on the crystal structure of piperidine, Chem. Cent. J. 9 (1) (2015), https://doi.org/10.1186/s13065-015-0086-3.
[20] Y. Kondo, S. Alavi, K. Murayama, et al. Effect of help-guest size and hydrogen bonding on the stability of N-methylpiperidine structure h clathrate hydrate. J. Phys. Chem. C 2020, 124(11), 5978–5986. https://www.x-mol.com/paperRedirect/1232073558833778688.
[21] G.J. Piermarini, S. Block, J.D. Barnett, et al. Calibration of the pressure dependence of the r1 ruby fluorescence line to 195 kbar. J. Appl. Phys. 1975, 46(6), 2774–2780. doi:https://doi.org/10.1063/1.321957.
[22] C.S. Yuan, X. Zhang, L.J. Zhou, et al. Phase transitions of carbon tetrachloride under static and dynamic pressures. J. Mol. Liq. 2021, 328, 115444. doi:https://doi.org/10.1016/j.molliq.2021.115444.
[23] A.D. Phan, A. Jedrzejowska, M. Paluch, et al., Theoretical and experimental study of compression effects on structural relaxation of glass-forming liquids, ACS Omega 5 (19) (2020) 11035–11042, https://doi.org/10.1021/acsomega.0c00860.
[24] C.M. Roland, S. Hensel-Bielowka, M. Paluch, et al., Supercooled dynamics of glass-forming liquids and polymers under hydrostatic pressure, Rep. Prog. Phys. 68 (2005) 1405, https://doi.org/10.1088/0034-4885/68/6/R03.
[25] M. Paluch, S.J. Rzoska, P. Habdas, et al., On the isothermal pressure behaviour of the relaxation times for supercooled glass-forming liquids, J. Phys. Condens. Matter 10 (1998) 4131, https://doi.org/10.1088/0953-8984/10/19/001.
[26] E.C. Dybeck, D.P. McMahon, G.M. Day, et al., Exploring the multi-minima behavior of small molecule crystal polymorphs at finite temperature, Cryst. Growth Des. 19 (10) (2019) 5568–5580, https://doi.org/10.1021/acs.cgd.9b00476.
[27] H. Yang, K. Shi, X. Dong, et al., Programmable compressing and decompressing for controllable polymerization: the case of methyl methacrylate, J. Phys. Chem. C 127 (34) (2023) 16929–16937, https://doi.org/10.1021/acs.jpcc.3c04439.
[28] C.S. Yuan, J. Wang, X. Zhang, et al. Influence of dynamic compression on the phase transition of cyclohexane. J. Mol. Liq. 2022, 363, 119836. doi:https://doi.org/10.1016/j.molliq.2022.119836.
[29] A. Sivakumar, S. Sahaya Jude Dhas, S. Chakraborty, et al. Dynamic shock wave-induced amorphous-to-crystalline switchable phase transition of lithium sulfate. J. Phys. Chem. C 2022, 126(6), 3194–3201. doi:https://doi.org/10.1021/acs.jpcc.1c09411.
[30] H. Voetter, H. Tschamler, Die molekülspektren gesättigter sechserringe, Monatsh. Chem. 84 (1953) 134–155, https://doi.org/10.1007/BF00899131.